

NJC

Accepted Manuscript



This is an *Accepted Manuscript*, which has been through the Royal Society of Chemistry peer review process and has been accepted for publication.

Accepted Manuscripts are published online shortly after acceptance, before technical editing, formatting and proof reading. Using this free service, authors can make their results available to the community, in citable form, before we publish the edited article. We will replace this *Accepted Manuscript* with the edited and formatted *Advance Article* as soon as it is available.

You can find more information about *Accepted Manuscripts* in the [Information for Authors](#).

Please note that technical editing may introduce minor changes to the text and/or graphics, which may alter content. The journal's standard [Terms & Conditions](#) and the [Ethical guidelines](#) still apply. In no event shall the Royal Society of Chemistry be held responsible for any errors or omissions in this *Accepted Manuscript* or any consequences arising from the use of any information it contains.

**Coordination Chemistry of Mixed M(Benzene)(Cyclopentadienyl) Sandwich
Complexes: Electronic Properties and Bonding Analysis**

Saber-Mustapha Zendaoui,^{a,b} Bachir Zouchoune^{*a,b}

^aLaboratoire de Chimie appliquée et Technologie des Matériaux, Université Larbi Ben M'Hidi-Oum El Bouaghi, (04000) Oum El Bouaghi, Algeria.

^bUnité de Recherche de Chimie de l'Environnement et Moléculaire Structurale, Université de Constantine, (25000) Constantine, Algeria.

E-mail: b.zouchoune@univ-oeb.dz, Phone: +213 6 62038183, Fax: +213 32 423983

Abstract

DFT calculations using BP86 and B3LYP functionals have been carried out for all the low-energy structures of mixed $[M(\text{Bz})\text{Cp}]^{+1/0/-1}$ ($M = \text{Ti-Ni}$) sandwich complexes of benzene and cyclopentadienyl ligands. The electronic configuration of cationic, neutral and anionic metal-ligand complexes and their structures are discussed, where depending on the metal nature, the spin state and the metal valence electrons, a complete rationalization of the bonding has been provided for the $[M(\text{Bz})\text{Cp}]^{+1/0/-1}$ complexes. The benzene and cyclopentadienyl adopt unchanged η^6 and η^5 hapticities, respectively, for Sc, Ti, V, Cr and Mn complexes, but various coordination modes for Fe, Co and Ni were emphasized, according to the metal oxidation state and the complex's spin state, where some of them involving full or partial coordination of either the benzene or of the cyclopentadienyl satisfying the metal electron demand. The ionization energy and the electron affinity showed that the neutral 19-electron iron complex is the easiest oxidized and reduced species among all the studied complexes.

***corresponding author**

1. Introduction

The breakthrough of the ferrocene in 1951,^{1,2} has given rise to wide investigations of more metallocenes with various transition metals in both experimental and theoretical fields.³ Since the pioneering work of Fischer and Hafner regarding sandwich π coordination of benzene and substituted benzene,⁴ the chemistry of discrete benzene π complexes has been developed extensively.^{5,6} The coordination chemistry of sandwich complexes containing benzene and their stabilities were understood by means of the familiar 18-electron rule. Likewise to the benzene sandwich complexes, those of cyclopentadienyl were widely explored, where Fischer and Hafner were the first to report a synthesis for chromocene,⁷ whose structure has been verified by X-ray diffraction several years hereafter,⁸ while the paramagnetic vanadocene has been highlighted by Müller et al.⁹

Nevertheless, that combined both ligands in sandwich manner is scarcely investigated, where few examples are experimentally known, particularly those of iron complexes serving as electron reservoirs with high redox potential^{10,11} and some substituted of ruthenium¹²⁻¹⁴ and cobalt¹⁵ metal complexes. However, the complexes of early metals are not explored apart from the vanadium case¹⁶, thereby, by this study we will intend to counter in this deficiency.

Some of the early theoretical works on neutral Fe(Bz)Cp complex considered as electron reservoirs were performed by Saillard et al.¹⁷ using local spin-density approximation to the density functional theory.

To date, the major theoretical studies have been focused on iron complexes and their derivatives; we will endeavor to extend our investigation over the 3d transition metal series, in order to provide a deeper insight regarding the coordination and electronic behavior of mixed benzene and cyclopentadienyl complexes based on the nature and the valence electrons of different 3d metals. The DFT method using BP86 and B3LYP has proven to be valuable in determining the electronic structure and bonding analysis for related organometallic compounds.^{30,31,18-26}

2. Computational methods

Density functional theory (DFT) calculations were carried out on the studied compounds using the Amsterdam Density Functional (ADF) program,²⁷ developed by Baerends and coworkers.²⁸⁻³² Electron correlation was treated within the local density approximation (LDA) in the Vosko-Wilk-Nusair parametrization.³³ The non-local corrections of Becke and Perdew (BP86) were added to the exchange and correlation energies, respectively.³⁴⁻³⁵ All the geometries discussed in this paper have been optimized at the BP86 and the hybrid-type

B3LYP functional (Becke's three parameter hybrid exchange functional³⁸ coupled with Lee-Yang-Parr nonlocal correlation functional).³⁹

The numerical integration procedure applied for the calculations was developed by te Velde et al.³² The atom electronic configurations were described by a triple- ζ Slater-type orbital (STO) basis set for H 1s, C 2s and 2p, N 2s and 2p augmented with a 3d single- ζ polarization for C and N atoms and with a 2p single- ζ polarization for H atoms. A triple- ζ STO basis set was used for the first row transition metals 3d and 4s augmented with a single- ζ 4p polarization function. A frozen-core approximation was used to treat the core shells up to 1s for C, N and 3p for the first row transition metals.²⁸⁻³² Full geometry optimizations were carried out using the analytical gradient method implemented by Versluis and Ziegler.⁴⁰ Spin-unrestricted calculations were performed for all the open-shell systems. Frequencies calculations^{41,42} were performed on all the studied compounds to check that the optimized structures are at local minima on the potential surface of energy. All the energy values reported in this paper include zero-point energy (ZPE) correction taken out from these frequency calculations. Representation of the molecular orbitals and molecular structures were done using ADF-GUI²⁷ and MOLEKEL4.1,⁴³ respectively.

3. Results and discussion

The benzene and the cyclopentadienyl ligands as formally neutral and monoanionic ligands, respectively, are potential donors of 6 π -electrons but the number of electrons effectively shared with the metal depends on the coordination mode and consequently can be lower or equal to 6. Therefore, we will use in the two following different electron counts for the investigated M(Bz)(Cp) compounds. (1) The total number of electrons (TNE) which is indicative of the global electron richness of the molecule, defined as the sum of all the electrons which can be potentially donated by the benzene and the cyclopentadienyl monoanion ligands (i.e., $2 \times 6 = 12$) besides the metal valence electrons in its actual oxidation state. Thus, $TNE = 2 \times 6 + n$ for a neutral Co(Bz)Cp complex, with n being the number of valence electrons of Co(I), thus, $TNE = 20$. (2) The number of metal valence electrons (MVE) which corresponds to the number of electrons really belonging to the metallic sphere. This number takes into account the ligand electrons which are effectively donated to the metal and consequently depends on the metal hapticity. For example in the case of Co(η^4 -Bz) (η^5 -Bz) where only four carbon atoms of the benzene ring and all the five atoms of the cyclopentadienyl are bonded to Co(I), therefore $MVE = 4 + 6 + 8 = 18$, whereas $TNE = 20$. MVE is necessarily

always lower or equal to TNE. The obtained results of the studied compounds will be presented according to the increasing order of the total number of electrons (TNE).

3.1. Scandium and titanium complexes

The Sc(Bz)Cp and [Ti(Bz)Cp]⁺ species having 14-TNE are the less electron riches of the studied M(Bz)Cp series for the first row transition metals. The [Sc(Bz)Cp] complex have been optimized in their singlet and triplet spin states, giving rise to the perfect η^6, η^5 coordination mode to the benzene and the cyclopentadienyl ligands, respectively, as shown in Fig. 1 and summarized in Table 1. For this deficient 14-MVE complex of Sc(I) metal cation, the triplet state is calculated more stable than that of the singlet one despite its significant HOMO-LUMO gap of 0.76 eV (BP86) or 2.14 eV (B3LYP). The electron deficiency is related to the vacant bonding M-L orbital (LUMO), thus, the occupation of this orbital suggests Sc-C(Bz) bond distances shortening with respect to the in-phase character between the metal and the benzene ring. Indeed, the Sc(Bz)Cp triplet spin state is calculated more stable by 5.6 kcal/mol (BP86) or 2.0 kcal/mol (B3LYP) than that of the singlet one, in which the obtained average Sc-C(Bz) bond distance of 2.435 Å (BP86) or 2.429 Å (B3LYP) is slightly short than that of the average Sc-C(Cp) of 2.489 Å (BP86) or 2.496 Å (B3LYP), respectively. The oxidized [Sc(Bz)Cp]⁺ species obtained by one electron removing from a Sc-C(Bz) bonding orbital (Figure 2) conducts obviously to bond distances lengthening as shown in (Table 1), where the average bond distance is equal to 2.533 Å (BP86) or 2.556 Å (B3LYP), However, the reduced [Sc(Bz)Cp]⁻ species obtained by one electron population of a Sc-C(Bz) bonding orbital Fig. 2, leads to bond distances shortening 2.378 Å (BP86) or 2.361 Å (B3LYP)). The same trends are observed for the isoelectronic [Ti(Bz)Cp]⁺ singlet spin structure exhibiting a small but a significant HOMO-LUMO of 0.78 eV (BP86) or large 2.58 one (B3LYP), giving rise to the perfect η^6, η^5 coordination mode with the average Ti-C(Bz) and Ti-C(Cp) bond distances 2.327 Å (BP86) or 2.387 Å (B3LYP) and 2.333 Å (BP86) or 2.337 Å (B3LYP), respectively. The [Ti(η^6 -Bz)(η^5 -Cp)]⁺ singlet state is calculated less stable than its homologous triplet one by 5.2 kcal/mol (BP86) or 6.3 kcal/mol (B3LYP). For the [Ti(η^6 -Bz)(η^5 -Cp)]⁺ triplet state, one can observe the lengthening of the Ti-C(9) and Ti-C(10) bond distances in accordance with the one electron depopulation of the Ti-Cp bonding HOMO, but the shortening of Ti-C(7), Ti-C(8) and Ti-C(11), in agreement with the one electron population of the Ti-Cp bonding LUMO (Fig. 2). The one and two electron successive reductions of the [Ti(η^6 -Bz)(η^5 -Cp)]⁺ species, give rise to the Ti(η^6 -Bz)(η^5 -Cp)

and $[\text{Ti}(\eta^6\text{-Bz})(\eta^5\text{-Cp})]^-$ doublet and singlet spin structures with 15- and 16-TNE, respectively, whose Ti-C(Bz) bond distances are short compared to those of 14-TNE consistent with the bonding orbital of 15- and 16-MVE species corresponding to fully coordinated benzene and cyclopentadienyl rings, for which the Ti-C(Bz) bond distances are clearly shortened, while

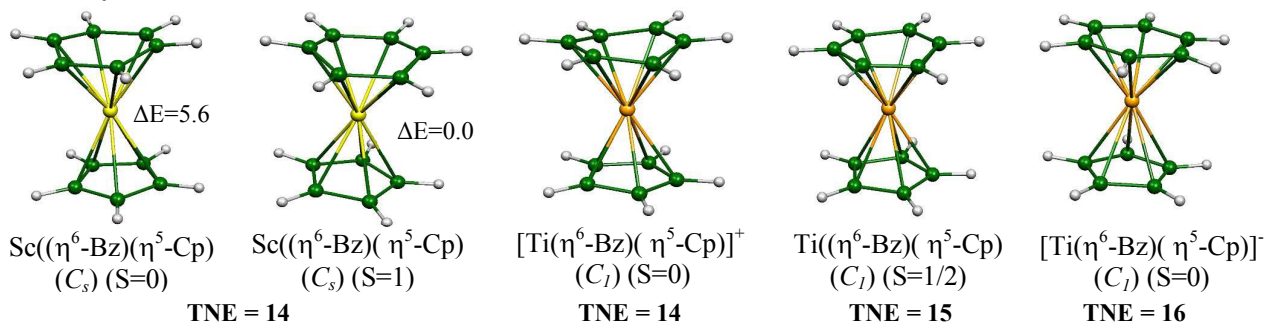


Fig. 1 Optimized geometries for $\text{Sc}(\text{Bz})\text{Cp}$, $[\text{Ti}(\text{Bz})\text{Cp}]^+$, $\text{Ti}(\text{Bz})\text{Cp}$ and $[\text{Ti}(\text{Bz})\text{Cp}]^-$ complexes. The relative energies between isomers are given in (kcal/mol).

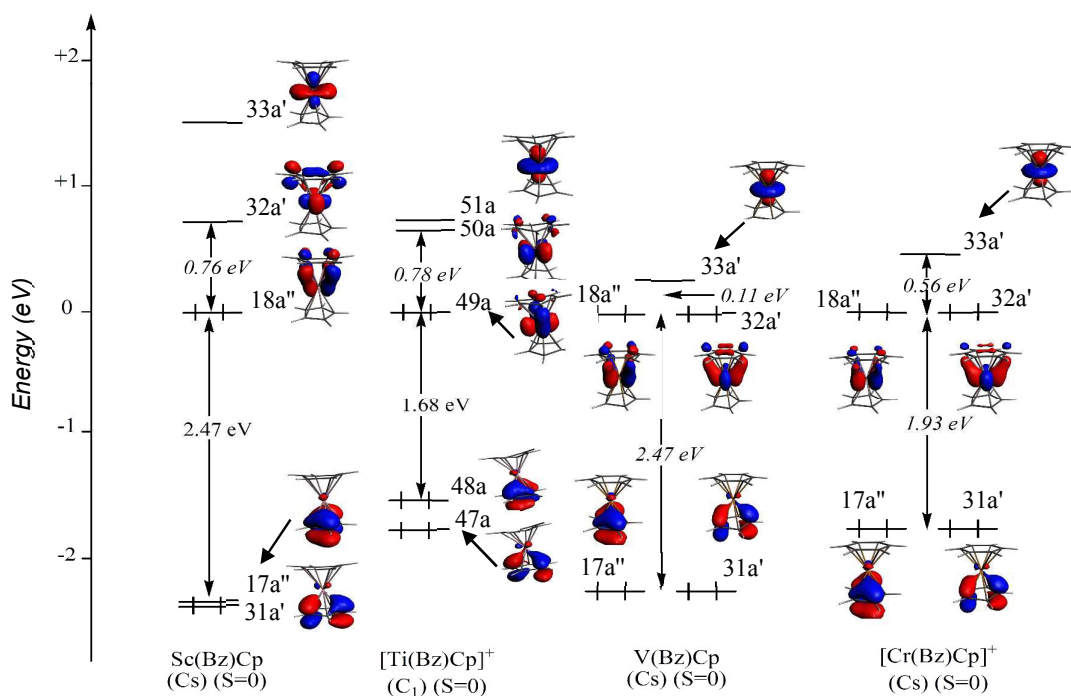


Fig. 2 MO diagrams of $\text{M}(\eta^6\text{-Bz})\text{Cp}$ ($\text{M} = \text{Sc}, \text{V}$) and $[\text{M}(\eta^6\text{-Bz})\text{Cp}]^+$ ($\text{M} = \text{Ti}, \text{Cr}$) complexes.

those corresponding to Ti-C(Cp) remain almost unchanged (Table 1). Thus, the singly and doubly occupations of the LUMO for the $[\text{Ti}(\eta^6\text{-Bz})(\eta^5\text{-Cp})]^+$ complex should reinforce the M-C(Bz) bond distances, it is what one can observe from the Table 1. The large HOMO-LUMO gaps obtained by B3LYP are comparable to the related complexes studied previously.²⁴⁻²⁶

Table 1 Selected parameters obtained for various $[M(\text{Bz})\text{Cp}]^{+1,0,-1}$ ($M = \text{Sc}, \text{Ti}$) complexes. The $\Delta(\text{HL})_1$ and $\Delta(\text{HL})_2$ HOMO-LUMO gaps are given in (kcal/mol), the $(\Delta E)_1$ and $(\Delta E)_2$ relative energies are given in (eV) and the bond distances are given in (Å).

	$[\text{Sc}(\text{Bz})\text{Cp}]^+$	$\text{Sc}(\text{Bz})\text{Cp}$		$[\text{Sc}(\text{Bz})\text{Cp}]^-$	$[\text{Ti}(\text{Bz})\text{Cp}]^+$		$\text{Ti}(\text{Bz})\text{Cp}$	$[\text{Ti}(\text{Bz})\text{Cp}]^-$	
TNE	13	14	14	15	14	14	15	16	16
MVE	13	14	14	15	14	14	15	16	16
Coordination mode	(η^6, η^5)	(η^6, η^5)	(η^6, η^5)	(η^6, η^5)	(η^6, η^5)	(η^6, η^5)	(η^6, η^5)	(η^6, η^5)	(η^6, η^5)
Symmetry	(C_s)	(C_s)	(C_s)	(C_s)	(C_i)	(C_i)	(C_i)	(C_i)	(C_i)
Spin state	$S = 1/2$	$S = 0$	$S = 1$	$S = 1/2$	$S = 0$	$S = 1$	$S = 1/2$	$S = 0$	$S = 1$
$\Delta(\text{HL})_1$ (BP86)	-	0.76	-	-	0.78	-	-	0.74	-
$\Delta(\text{HL})_2$ (B3LYP)	-	2.14	-	-	2.58	-	-	2.39	-
$(\Delta E)_1$ (BP86)	-	5.6	0.0	-	5.2	0.0	-	0.0	4.5
$(\Delta E)_2$ (B3LYP)	-	2.0	0.0	-	6.3	0.0	-	0.0	0.2
Average M-C(Bz) ¹	2.553	2.439	2.435	2.378	2.327	2.387	2.273	2.218	2.220
Average M-C(Bz) ²	2.556	2.397	2.429	2.361	2.387	2.416	2.276	2.227	2.226
Average M-C(Cp) ¹	2.428	2.480	2.489	2.536	2.333	2.334	2.346	2.370	2.369
Average M-C(Cp) ²	2.438	2.498	2.496	2.536	2.337	2.342	2.373	2.392	2.374
Metal spin density	0.67	-	1.02	0.44	-	1.63	0.72	-	1.81
$\langle S^2 \rangle$	0.75	-	2.00	0.75	-	2.00	0.76	-	2.01
Hirshfeld metal charge	0.54	0.40	0.38	0.26	0.45	0.42	0.31	0.21	0.12

¹Bond distances obtained by BP86.

²Bond distances obtained by B3LYP.

3.2. Vanadium and chromium complexes

The neutral $V(Bz)(Cp)$ 16-TNE sandwich complexes were optimized in their singlet and triplet spin states showing a perfect η^6, η^5 coordination mode of the benzene and cyclopentadienyl rings, respectively, giving rise to deficient 16-MVE species as displayed in (Fig. 3). The global minimum $V(\eta^6-Bz)(\eta^5-Cp)$ corresponds to the triplet state structure which is calculated more stable than the singlet state one by 18.7 kcal/mol (BP86) or 21.1 kcal/mol (B3LYP), reproducing the paramagnetic behavior of the experimental structure.¹⁶ The obtained geometrical parameters are summarized in Table 2. The findings show a discrepancy with regard to those of the isoelectronic $[Ti(Bz)(Cp)]^-$ giving the singlet spin state more stable than the triplet one and exhibits relatively large HOMO-LUMO gap of 0.74 eV (BP86) or 2.10 eV (B3LYP) (Fig. 2). One can see the comparable findings between those of the triplet and the experimental ones, where the average V-C(Bz) and V-C(Cp) bond distances are of 2.254 Å (BP86) or 2.262 Å (B3LYP) and 2.226 Å (BP86) or 2.307 Å (B3LYP), respectively. The MO diagram for the $[V(\eta^6, \eta^5-Bz)_2]$ closed-shell model exhibits a small HOMO-LUMO gap of 0.11 eV (BP86), in accordance with its relative instability according to the triplet structure. The passage from the singlet structure to the triplet one is not accompanied by structural modifications due to the purely metallic character of the populated orbital ($33a'$) as sketched in (Fig. 2). The $[Cr(Bz)Cp]^+$ 16-TNE complex is electronically equivalent to $V(Bz)Cp$. The main structural and energy parameters calculated for the neutral, oxidized and reduced of chromium species are given in Table 2. The $[Cr(Bz)Cp]^+$ exhibits similar trends compared to the $V(Bz)Cp$ one concerning relative stability, HOMO-LUMO gap and bond distances evolution. The $[Cr(Bz)Cp]^+$ oxidized singlet spin state structure of C_s symmetry displays a small HOMO-LUMO gap of 0.56 eV (BP86), but a relatively large one of 1.57 eV (B3LYP) predicting low-lying triplet and quintet spin state structures. Indeed, the $[Cr(\eta^6-Bz)(\eta^5-Cp)]^+$ triplet is obtained as a global minimum lying 32.2 kcal/mol or 25.7 kcal/mol (B3LYP) below its homolog of singlet spin state, featuring short and comparable average Cr-C(Bz) and Cr-C(Cp) bond distances of 2.217 Å (BP86) or 2.246 Å (B3LYP) and 2.201 Å (BP86) or 2.209 Å (B3LYP), respectively. The neutral $Cr(Bz)Cp$ species is optimized in its doublet spin state with C_s symmetry, where the energy minimum structure corresponds to a perfect η^6, η^5 coordination mode arising from strong interactions between chromium and both monocyclic ligands as evidenced by short averaged Cr-C(Bz) and Cr-C(Cp) bond lengths of 2.124 Å (BP86) or 2.143 Å (B3LYP) and 2.183 Å (BP86) or 2.207 Å (B3LYP), respectively. The one electron reduction of the neutral $Cr(Bz)Cp$ conducts to the

$[\text{Cr}(\text{Bz})\text{Cp}]^-$ model possessing 18-MVE, which is electronically equivalent to the characterized dibenzene chromium $\text{Cr}(\text{Bz})_2$ structure. The reduced structure exhibits slight Cr-C(Bz) and Cr-C(Cp) bond distances shortening as gathered in Table 2, in accordance with the localization of the involved orbital (Fig. 2). The anionic $[\text{Cr}(\text{Bz})\text{Cp}]^-$ is electronically equivalent to the alkylated dibenzenechromium $[\text{Me}_2\text{Cr}(\text{Bz})_2]$ experimentally characterized complex as a sandwich monometallic species of the benzene ligand, which exists as eclipsed conformer of D_{6h} symmetry.⁴⁴⁻⁴⁶ The 18-MVE rule requires to the benzene and cyclopentadienyl anion to provide all their 12 π electrons to the Cr(0) (d^6) metal centre. It is worth noting that the barrier rotation energy does not exceed 1.0 kcal/mol, thereby, no significant modifications stemmed from rotation between benzene and cyclopentadienyl rings, agreeing well with previous works.

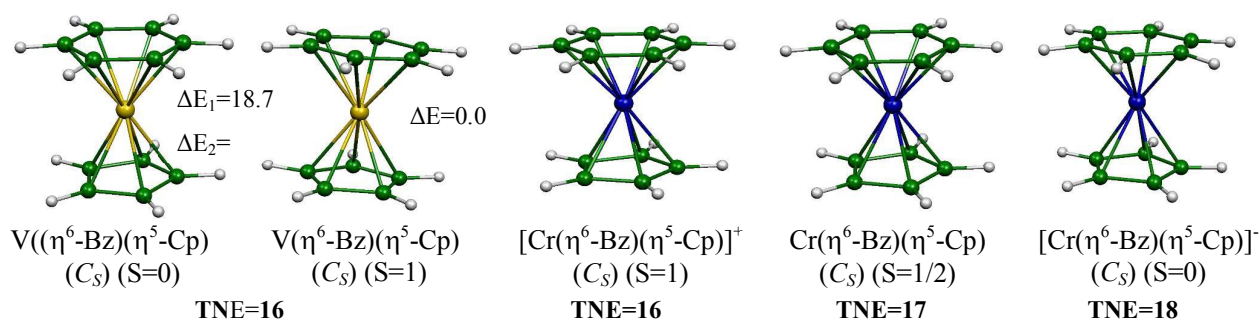


Fig. 3 Optimized geometries for $\text{V}(\text{Bz})\text{Cp}$, $[\text{Cr}(\text{Bz})\text{Cp}]^+$, $\text{Cr}(\text{Bz})\text{Cp}$ and $[\text{Cr}(\text{Bz})\text{Cp}]^-$ complexes. The relative energies between isomers are given in kcal/mol.

3.3. Manganese and iron complexes

Full geometry optimizations have been carried out on the neutral $\text{Mn}(\text{Bz})\text{Cp}$ 18-TNE and $\text{Fe}(\text{Bz})\text{Cp}$ 19-TNE, their oxidized and reduced derivatives as shown in (Fig. 4). The neutral $\text{Mn}(\text{Bz})\text{Cp}$ singlet state is found as the global minimum, where the metal is coordinated in η^6 and η^5 to the benzene and cyclopentadienyl ligands, respectively. As results, the $\text{Mn}(\text{Bz})\text{Cp}$ exhibits a very large HOMO-LUMO gap of 2.59 eV (BP86) or 4.46 eV (B3LYP) (Fig. 5 and Table 3) satisfying the 18-electron rule, in accordance with the cationic Mn(I) center and forecasting a high-lying triplet spin state structure. Indeed, the triplet structure is found 9.7 kcal/mol (BP86) or 11.3 kcal/mol (B3LYP) above the singlet one. This relative stability matches very well with the Mn-C bond distances modifications, where those of Mn-C(Bz) are lengthened by 0.11 Å and those of Mn-C(Cp) by an average value of about 0.15 Å. Depopulation of the bonding metal-ligand induces some lengthening of the Mn-C(Bz) bond distances, while the Mn-C(Cp) ones remain almost unchanged due to the no contribution

of the Cp to this orbital (33a'). It is worth noting that the findings obtained for the neutral Mn complex follow the same tendencies than those of the isoelectronic Cr anion regarding the large HOM-LUMO gap and stability order between singlet and triplet isomers. It is interesting to note that the neutral, oxidized and reduced species keep the same η^6, η^5 coordination mode, but with some geometrical modifications, particularly those of the reduced one showing Mn-C bond distances lengthening (Table 3) due to the antibonding Mn-C character of the 34a' orbital, particularly between Mn and Cp ligand. The same tendencies were obtained for the rhenium species whose results are not discussed here. The neutral Fe(Bz)Cp 19-TNE species is optimized in its doublet state showing a full coordination of both benzene and cyclopentadienyl ligands to the iron center. Indeed, the $\text{Fe}(\eta^6\text{-Bz})(\eta^5\text{-Cp})$ with 19-MVE corresponds to a structure exhibiting short Fe-C(Bz) and Fe-C(Cp) bond distances with averaged values of 2.136 Å (BP86) or 2.168 Å (B3LYP) and 2.188 Å (BP86) or 2.219 Å (B3LYP), respectively, comparable to those obtained experimentally for the substituted $\text{Fe}(\eta^6\text{-C}_6\text{Me}_6)(\eta^5\text{-Cp})$.¹¹ One can observe that the computed Fe-C(Bz) bond lengths are relatively longer than those between the iron and the Cp ligand. The Fe(I) as mono-cation attains the 19-MVE configuration, where the extra electron is located in the SOMO metal-ligand based on the metal contribution evaluated to 57% (Fig. 5), a value which is higher than the substituted species as evidenced by previous work.⁴⁷ the unpaired electron is located in the SOMO 34a' orbital highlighted by the spin density value of 0.95 (BP86). The oxidized $[\text{Fe}(\text{Bz})\text{Cp}]^+$ complex obtained by one electron removing from the SOMO keeps the same coordination mode in which the iron metal is dicationic Fe(II) center obeying the 18-MVE configuration (oxidation mechanism is given in Scheme 1). The one electron attachment of the neutral open-shell species gives the reduced $[\text{Fe}(\text{Bz})\text{Cp}]^-$ closed-shell structure which undergoes a decoordination of the benzene ring from η^6 to η^5 evidenced by the lengthening of the Fe-C(4) bond distance from 2.193 to 2.763 Å (BP86), thus, giving a distorted bent structure. This situation gives to the $[\text{Fe}(\eta^6\text{-Bz})(\eta^5\text{-Cp})]^-$ structure the iron metal as Fe(0) center the 20-MVE configuration, where the two extra electrons are located in the Fe-C antibonding orbital for the singlet structure. The $[\text{Fe}(\eta^6\text{-Bz})(\eta^2\text{-Cp})]^-$ triplet spin corresponds to the ground state lying 18.4 kcal/mol or 8.4 kcal/mol (B3LYP) below the singlet one. Unlike to the singlet structure, the $[\text{Fe}(\text{Bz})\text{Cp}]^-$ triplet structure exhibits η^6, η^2 coordination mode showing a partial η^2 hapticity of cyclopentadienyl related to three Fe-C distances of 2.618, 2.820 and 2.618 Å. For the $[\text{Fe}(\text{Bz})\text{Cp}]^-$ triplet structure, both the unpaired electrons are located on the metal center corresponding to the neutral Fe(0) as evidenced clearly by the Fe

spin density value of 2.10 and a spin contamination $\langle S^2 \rangle$ value of 2.03. The calculated net charge of Fe(0) of 0.02 is consistent with the metal zerovalent center acquiring the deficient 16-MVE configuration. It is interesting to indicate that the rotation barrier does not exceed 1.0 kcal/mol, a value which is not significant at the considered level of theory.

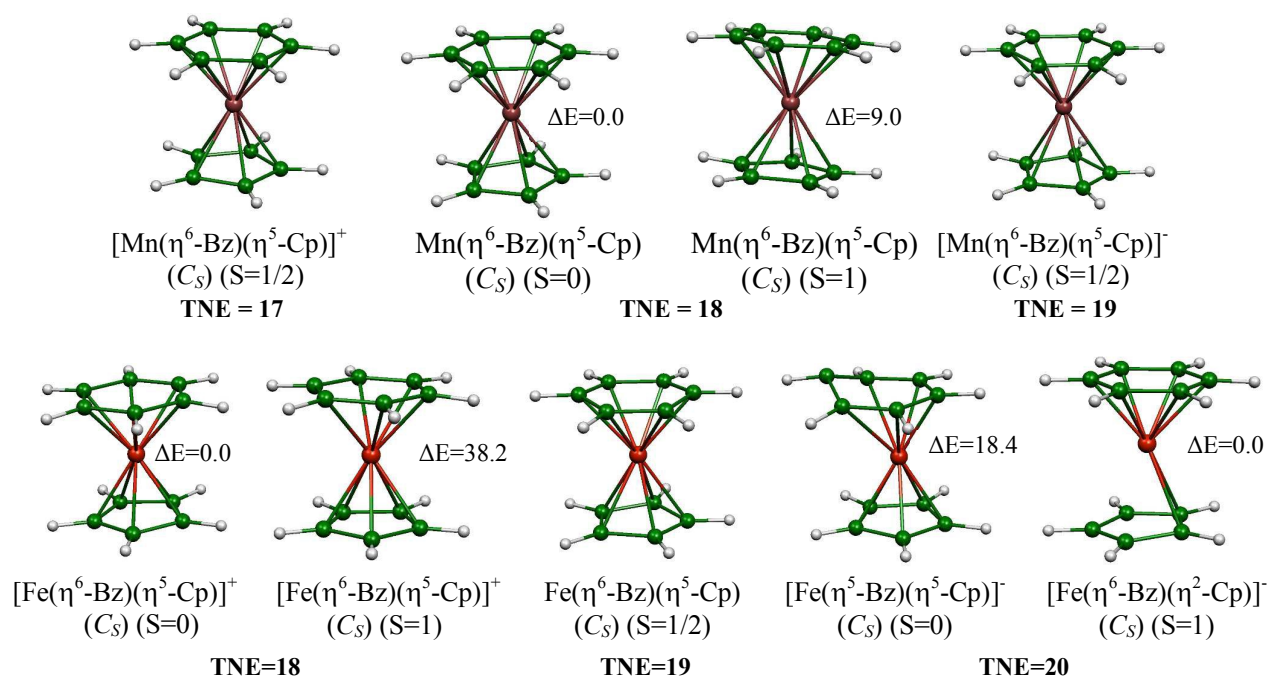


Fig. 4 Optimized geometries for $[M(\text{Bz})\text{Cp}]^{+1/0/-1}$ (M = Mn, Fe) complexes. The relative energies between isomers are given in (kcal/mol).

Table 2 Selected parameters obtained for various $[M(\text{Bz})\text{Cp}]^{+1/0/-1}$ ($M = \text{V}, \text{Cr}$) complexes. The $\Delta(\text{HL})_1$ and $\Delta(\text{HL})_2$ HOMO-LUMO gaps are given in (kcal/mol), the $(\Delta E)_1$ and $(\Delta E)_2$ relative energies are given in (eV) and the bond distances are given in (Å).

	$[\text{V}(\text{Bz})\text{Cp}]^+$	$\text{V}(\text{Bz})\text{Cp}$		$[\text{V}(\text{Bz})\text{Cp}]^-$	$[\text{Cr}(\text{Bz})\text{Cp}]^+$		$\text{Cr}(\text{Bz})\text{Cp}$	$[\text{Cr}(\text{Bz})\text{Cp}]^-$	
TNE	15	16	16	17	16	16	17	18	18
MVE	15	16	16	17	16	16	17	18	18
Coordination mode	(η^6, η^5)	(η^6, η^5)	(η^6, η^5)	(η^6, η^5)	(η^6, η^5)	(η^6, η^5)	(η^6, η^5)	(η^6, η^5)	(η^6, η^5)
Symmetry	(C_s)	(C_s)	(C_s)	(C_s)	(C_s)	(C_s)	(C_s)	(C_s)	(C_s)
Spin state	$S = 1/2$	$S = 0$	$S = 1$	$S = 1/2$	$S = 0$	$S = 1$	$S = 1/2$	$S = 0$	$S = 1$
$\Delta(\text{HL})_1$ (BP86)	-	0.11	-	-	0.56	-	-	1.87	-
$\Delta(\text{HL})_2$ (B3LYP)	-	2.10	-	-	1.57	-	-	3.03	-
$(\Delta E)_1$ (BP86)	-	18.7	0.0	-	32.2	0.0	-	0.0	27.8
$(\Delta E)_2$ (B3LYP)	-	21.2	0.0	-	25.7	0.0	-	0.0	31.4
Average M-C(Bz) ¹	2.319	2.254	2.254 (2.225) ^d	2.172	2.130	2.217	2.124	2.115	2.161
Average M-C(Bz) ²	2.380	2.162	2.262	2.181	2.230	2.246	2.143	2.131	2.142
Average M-C(Cp) ¹	2.261	2.272	2.226 (2.240) ^d	2.277	2.173	2.201	2.183	2.164	2.141
Average M-C(Cp) ²	2.277	2.256	2.307	2.316	2.190	2.209	2.207	2.230	2.247
Metal spin density	1.02	-	2.04	1.28	-	2.24	1.31	-	2.39
$\langle S^2 \rangle$	1.68	-	2.03	0.77	-	2.04	0.78	-	2.14
Hirshfeld metal charge	0.30	0.12	0.18	0.10	0.51	0.49	0.40	0.25	0.35

¹Bond distances obtained by BP86.

²Bond distances obtained by B3LYP.

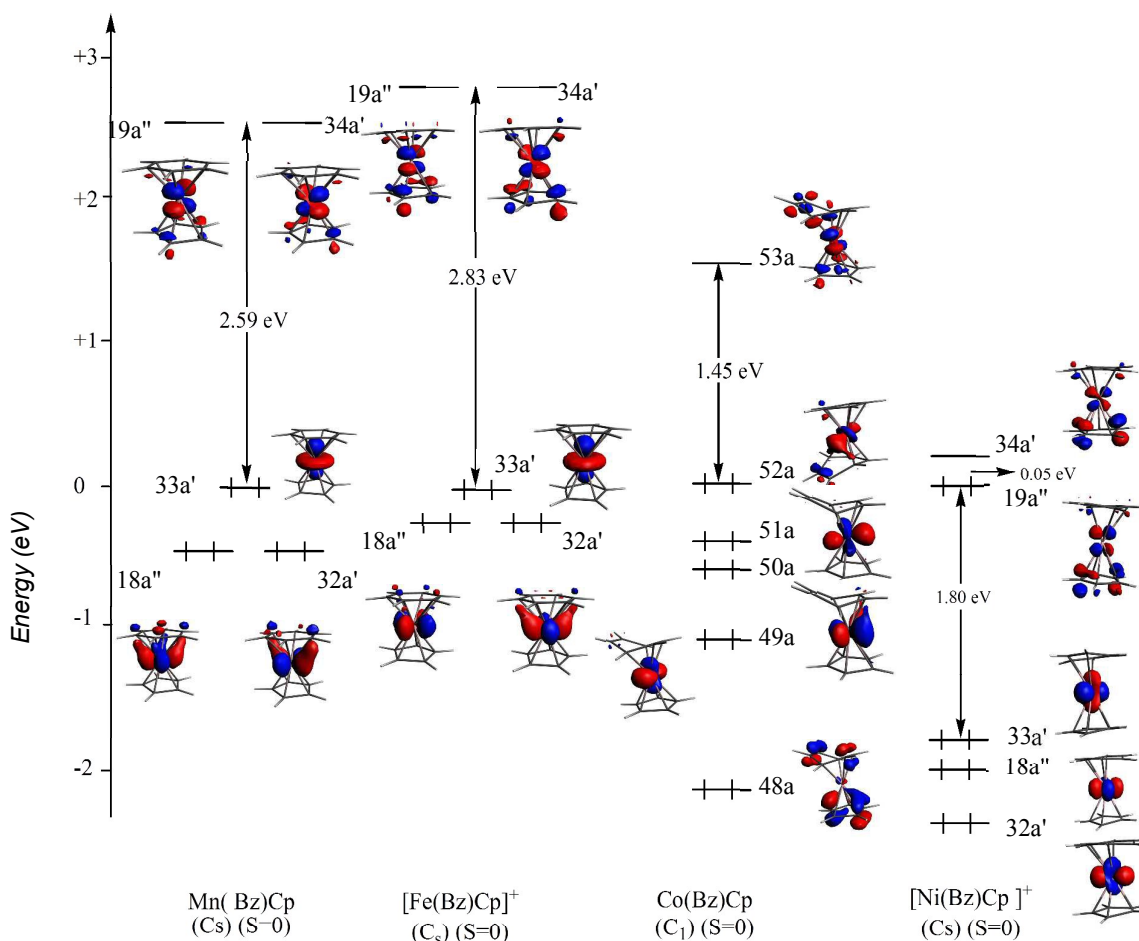


Fig. 5 MO diagrams of M(Bz)Cp (M = Mn, Co) and, [M(Bz)Cp]⁺ (M = Fe, Ni) complexes.

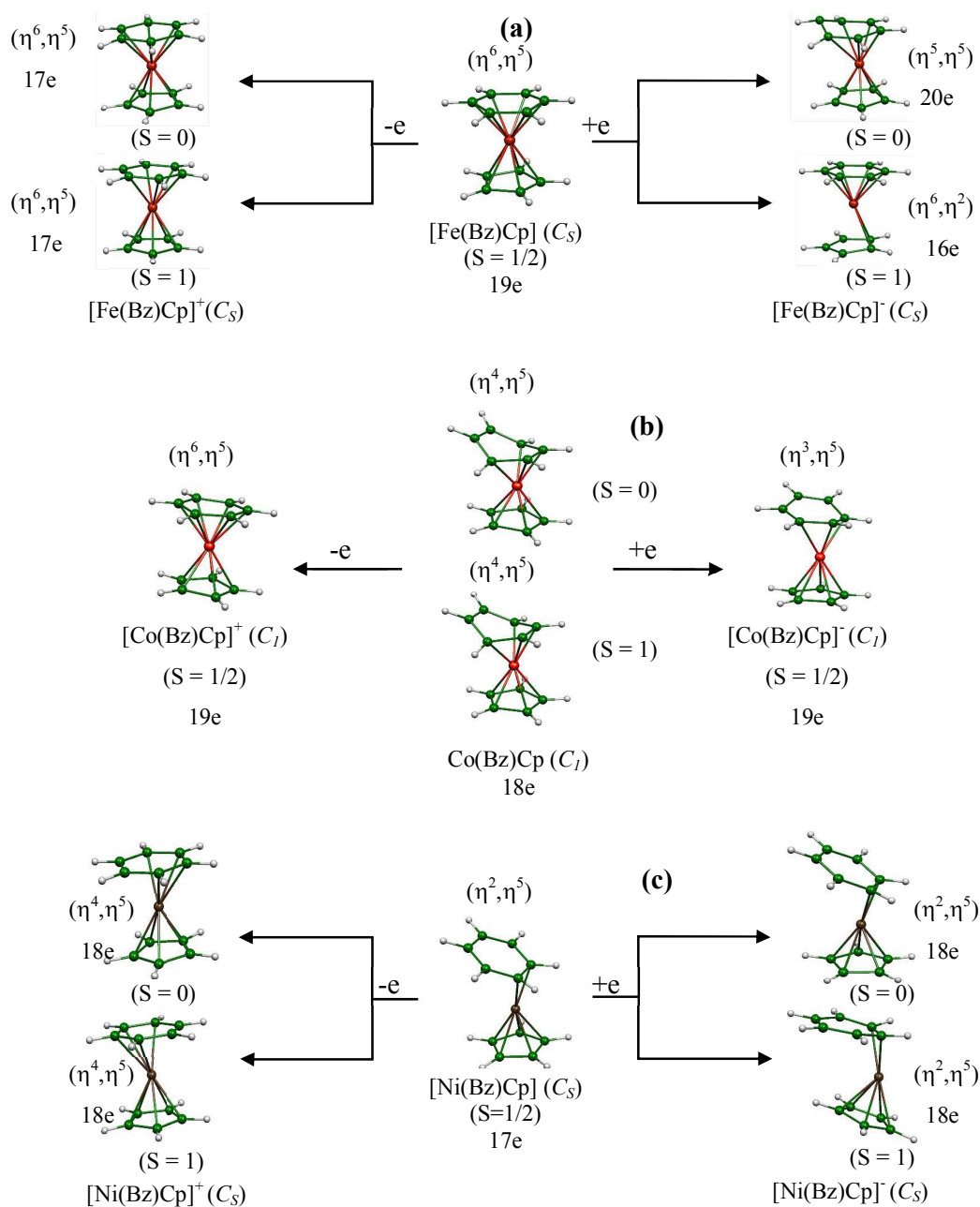
3.4. Cobalt and nickel complexes

Going from iron to cobalt is associated with one supplementary electron which should occupy a higher energy MO, particularly that of an M-L antibonding character. It is what happened, where a decoordination of the benzene ring from η^6 to η^4 has occurred giving rise to the Co(η^4 -Bz)(η^5 -Cp) structure (Fig. 4). The Co(η^4 -Bz)(η^5 -Cp) 20-TNE singlet structure exhibiting a large HOMO-LUMO gap of 1.45 eV (Table 4 and Fig. 5), leading to a cationic Co(I) center which fulfils the 18-MVE configuration. The Co(η^4 -Bz)(η^5 -Cp) triplet structure is found slightly less stable by 3.0 kcal/mol or 5.0 kcal/mol (B3LYP) than the singlet one. This weak difference in energy is reflected by the comparable bond distances between singlet and triplet structures as gathered in Table 4. It is worth noting that the geometrical parameters of singlet structure are comparable to those obtained experimentally for the substituted benzene ring species.¹⁵ The η^4 coordination mode is characterized by

Table 3 Selected parameters obtained for various $[M(\text{Bz})\text{Cp}]^{+1/0/-1}$ (M = Mn, Fe) complexes.

	$[\text{Mn}(\text{Bz})\text{Cp}]^+$	$\text{Mn}(\text{Bz})\text{Cp}$		$[\text{Mn}(\text{Bz})\text{Cp}]^-$	$[\text{Fe}(\text{Bz})\text{Cp}]^+$		$[\text{Fe}(\text{Bz})\text{Cp}]$	$[\text{Fe}(\text{Bz})\text{Cp}]^-$	
TNE	17	18	18	19	18	18	19	20	20
MVE	17	18	18	19	18	18	19	20	16
Coordination mode	(η^6, η^5)	(η^6, η^5)	(η^6, η^5)	(η^6, η^5)	(η^6, η^5)	(η^6, η^5)	(η^6, η^5)	(η^5, η^5)	(η^6, η^2)
Symmetry	(C_s)	(C_s)	(C_s)	(C_s)	(C_s)	(C_s)	(C_s)	(C_s)	(C_s)
Spin state	S = 1/2	S = 0	S = 1	S = 1/2	S = 0	S = 1	S = 1/2	S = 0	S = 1
$\Delta(\text{HL})_1$ (BP86)	-	2.59	-	-	2.83	-	-	0.33	-
$\Delta(\text{HL})_2$ (B3LYP)	-	4.46	-	-	5.12	-	-	1.90	-
$(\Delta E)_1$ (BP86)	-	0.0	9.0	-	0.0	38.2	-	18.4	0.0
$(\Delta E)_2$ (B3LYP)	-	0.0	11.3	-	0.0	19.2	-	8.4	0.0
Average M-C(Bz) ¹ (Å)	2.126	2.100	2.213	2.115	2.112	2.241	2.136	2.161	2.137
Average M-C(Bz) ² (Å)	2.254	2.268	2.315	2.337	2.139	2.358	2.168	2.219	2.220
Average M-C(Cp) ¹ (Å)	2.129	2.131	2.269	2.267	2.088	2.193	2.188	2.125	2.258
Average M-C(Cp) ² (Å)	2.157	2.133	2.273	2.312	2.089	2.217	2.219	2.168	2.243
Metal spin density	1.28	-	2.25	1.02	-	1.93	0.95	-	2.11
$\langle S^2 \rangle$	0.77	-	2.11	0.78	-	2.06	0.77	-	2.13
Hirshfeld metal charge	0.17	0.05	0.14	-0.02	0.10	0.20	0.05	-0.01	0.02

¹Bond distances obtained by BP86.²Bond distances obtained by B3LYP.



Scheme. 1 Oxidation and reduction mechanisms for neutral iron (a), cobalt (b) and nickel (c) complexes.

a slippage of the cobalt center towards the C(1), C(2), C(5) and C(5) carbon atoms of the benzene ring related to short Co-C(1), Co-C(2), Co-C(5) and Co-C(6) of 1.987, 2.079, 2.081 and 1.987 Å, against long Co-C(3) and Co-C(4) distances of 2.847 Å, matching well with the observed bond distances. For the triplet spin state structure, both unpaired electrons are localized on the cobalt metal as evidenced by the spin density values of 1.78 showing no spin

contamination inspired by the $\langle S^2 \rangle$ value of 2.04 comparable to the expected one of 2.00, thus conducting to reliable structure. The oxidized $\text{Co}(\eta^6\text{-Bz})(\eta^5\text{-Cp})$ species shows full coordination of both benzene and cyclopentadienyl ligands giving rise to 17-MVE complex, corresponding to a dicationic $\text{Co}(\text{II})$ center (Scheme 1b). The reduced $\text{Co}(\eta^3\text{-Bz})(\eta^5\text{-Cp})$ doublet state structure, where η^3 -allylic coordination is related to a zwitterionic form of the benzene, thus sharing four π -electrons with the $\text{Co}(0)$ metal attaining the 19-MVE configuration (Scheme 1b), where the unpaired electron is localized on the metal witnessed by the spin density value of 0.95 and $\langle S^2 \rangle$ of 0.76 (BP86) indicating the absence of spin contamination.

For the most rich $\text{Ni } d^{10}$ metal corresponding to 21-TNE complexes, the full geometry optimizations showed partial decoordination of the benzene ring (Fig. 4). Indeed, the neutral doublet spin state structure adopts an η^2, η^5 coordination mode highlighting a partial coordination of the benzene, but a total coordination of the cyclopentadienyl. This new coordination type provides a 17-MVE configuration to the $\text{Ni}(\text{I})$ cation acquiring a large positive Hirshfeld charge of +0.35 (Table 4), which matches well with the localization of the unpaired electron whose spin density is of 0.87 and the spin contamination value of $\langle S^2 \rangle = 0.75$ perfectly correlating with the expected value of 0.75. The two $\text{Ni-C}(\text{Bz})$ bond distances are of 2.045 Å (BP86) or 2.232 Å (B3LYP) between the metal and the complexed C-C double bond putting emphasis on the strong interactions, while the average bond distance between the nickel center and the cyclopentadienyl ring is of 2.171 Å (BP86) or 2.240 Å (B3LYP), which is somewhat longer than that between nickel and benzene ring, giving rise to a perfect η^5 coordination mode. The one electron oxidation of the neutral $\text{Ni}(\eta^2\text{-Bz})(\eta^5\text{-Cp})$ giving the cationic $[\text{Ni}(\eta^2\text{-Bz})(\eta^5\text{-Cp})]^+$, in which the nickel corresponds to $\text{Ni}(\text{II}) d^8$ center acquiring the 16-MVE configuration, in accordance with the tetrahedral ML_4 environment. The one electron reduction of the neutral $\text{Ni}(\eta^2\text{-Bz})(\eta^5\text{-Cp})$ gives the anionic $[\text{Ni}(\eta^2\text{-Bz})(\eta^5\text{-Cp})]^-$ species, in which the nickel corresponds to $\text{Ni}(0) d^{10}$ center satisfying the 18-electron rule. The one electron oxidation and the one electron reduction mechanisms are given in Scheme 1c.

Table 4 Selected parameters obtained for various $[M(\text{Bz})\text{Cp}]^{+1/0/-1}$ ($M = \text{Co}, \text{Ni}$) complexes.

	$[\text{Co}(\text{Bz})\text{Cp}]^+$	$\text{Co}(\text{Bz})\text{Cp}$		$[\text{Co}(\text{Bz})\text{Cp}]^-$	$[\text{Ni}(\text{Bz})\text{Cp}]^+$		$\text{Ni}(\text{Bz})\text{Cp}$	$[\text{Ni}(\text{Bz})\text{Cp}]^-$	
TNE	19	20	20	21	20	20	21	22	22
MVE	19	18	18	19	18	18	17	18	18
Coordination mode	(η^6, η^5)	(η^4, η^5)	(η^4, η^5)	(η^3, η^5)	(η^4, η^5)	(η^4, η^5)	(η^2, η^5)	(η^2, η^5)	(η^2, η^5)
Symmetry	(C_1)	(C_1)	(C_1)	(C_1)	(C_s)	(C_s)	(C_s)	(C_s)	(C_s)
Spin state	$S = 1/2$	$S = 0$	$S = 1$	$S = 1/2$	$S = 0$	$S = 1$	$S = 1/2$	$S = 0$	$S = 1$
$\Delta(\text{HL})_1$ (BP86)	-	1.45	-	-	0.05	-	-	1.72	-
$\Delta(\text{HL})_2$ (B3LYP)	-	3.25	-	-	1.25	-	-	3.01	-
$(\Delta E)_1$ (BP86)	-	0.0	3.0	-	2.3	0.0	-	0.0	40.3
$(\Delta E)_2$ (B3LYP)	-	0.0	5.0	-	0.0	2.9	-	0.0	20.7
Average M-C(Bz) ¹ (Å)	2.179	2.033(2.003) ^c	2.032	2.074	2.269	2.302	2.045	2.045	2.120
Average M-C(Bz) ² (Å)	2.263	2.058	2.143	2.120	2.274	2.315	2.232	2.058	2.104
Average M-C(Cp) ¹ (Å)	2.139	2.105(2.051) ^c	2.106	2.188	2.207	2.206	2.171	2.171	2.238
Average M-C(Cp) ² (Å)	2.162	2.146	2.293	2.273	2.226	2.238	2.240	2.194	2.247
Metal spin density	0.76	-	1.62	0.93	-	1.04	0.73	-	1.12
$\langle S^2 \rangle$	0.76	-	2.04	0.77	-	2.01	0.76	-	2.01
Hirshfeld metal charge	0.11	0.04	0.09	-0.01	0.39	0.42	0.34	0.20	0.23

¹Bond distances obtained by BP86.²Bond distances obtained by B3LYP.

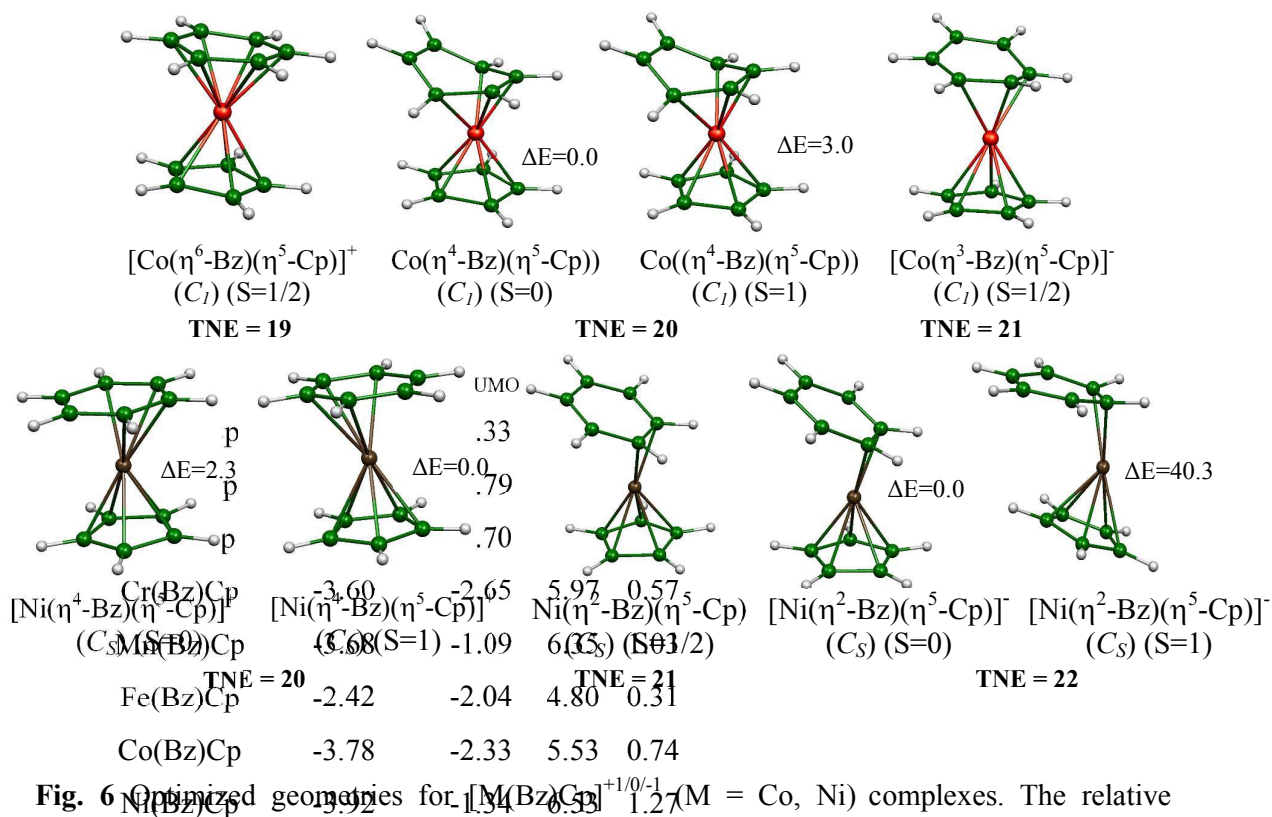


Fig. 6 Optimized geometries for $[M(\text{Bz})\text{Cp}]^{+1/0/-1}$ ($M = \text{Co}, \text{Ni}$) complexes. The relative energies between isomers are given in (kcal/mol).

4.5. Ionization energy and electron affinity

The ionization energy (IE) and electron affinity (EA) are important parameters for the understanding the stability towards the removing of one electron from HOMO and the attachment of one electron to LUMO, respectively. In the framework of this ongoing study, we were interested in determining the adiabatic ionization energy (AIE), which is the energy difference between the neutral and oxidized form for the optimized structures and AEA is the energy difference between neutral and anionic forms at their respective optimized geometries.

Table 5 Selected energetic parameters in (eV) of HOMO or SOMO, LUMO, adiabatic ionization energy and adiabatic electron affinity for various neutral M(Bz)Cp complexes.

Complex	$E_{\text{HOMO/SOMO}}$ (BP86)	E_{LUMO} (BP86)	AIE		AEA	
			BP86	B3LYP	BP86	B3LYP
Sc(Bz)Cp	-3.03	-2.33	5.42	5.12	0.47	0.10
Ti(Bz)Cp	-3.37	-2.79	5.60	5.25	0.75	0.39
V(Bz)Cp	-3.23	-2.70	5.67	4.95	0.82	0.41
Cr(Bz)Cp	-3.60	-2.65	5.97	5.48	0.57	0.27
Mn(Bz)Cp	-3.68	-1.09	6.35	5.75	0.42	0.25
Fe(Bz)Cp	-2.42	-2.04	4.80	4.87	0.31	0.23
Co(Bz)Cp	-3.78	-2.33	5.53	6.02	0.74	0.34
Ni(Bz)Cp	-3.92	-1.34	6.53	5.75	1.27	0.46

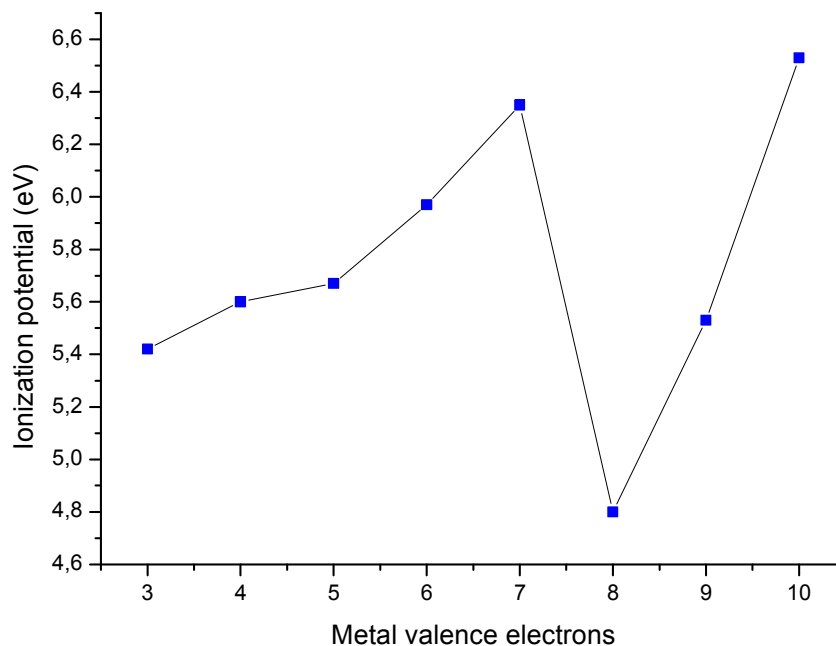


Fig. 7 Ionization energy (BP86) variation as function of metal valence electrons.

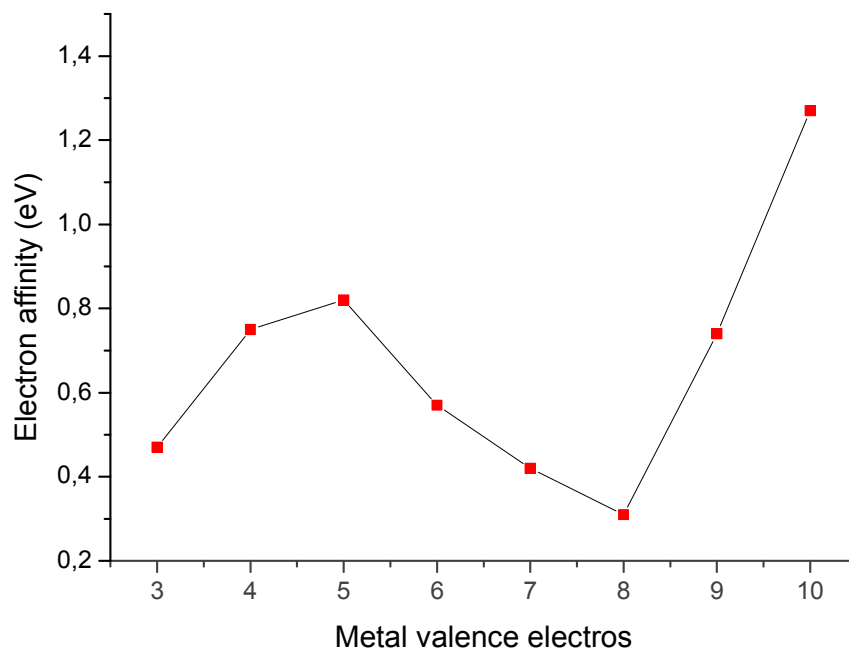


Fig. 8 Electron affinity (BP86) variation as function of metal valence electrons.

Since complexes generally relax following their ionization. The calculated AIE and AEA values of the optimized structures are summarized in Table 5 and presented in Figures 7 and 8, where the energy needed for removal and for attachment of an electron yields valuable information on the electronic structure.

The variation of the ionization energy (BP86) of $M(\text{Bz})\text{Cp}$ complexes is not uniformly enhanced when crossing the first row of transition metals, they exhibit different behaviours across the 3d series. Indeed, the ionization energy increase from Sc (5.42 eV) to Mn (6.35 eV) by about (1.0 eV), then decrease from Mn to Fe and increase From Fe to Co and Ni (Fig. 7). The same tendencies are obtained using (B3LYP) functional, but with values slightly weaker than those obtained by (BP86) as summarized in Table 5 except for the cobalt complex, where the trend is inverted. The variations in the ionization energies of $M(\text{Bz})\text{Cp}$ complexes across the 3d series can be understood by comparing their HOMO energy levels. Thereby, the smallest AIE value calculated for the iron 4.80 eV (BP86) or 4.77 eV (B3LYP) complex is correlated to higher HOMO energy; on the other hand, the largest one obtained for the nickel (6.51 eV) complex corresponds to the lower HOMO energy as summarized in Table 5. We can conclude that there is a perfect correlation between AIE values and HOMOs' energies and we can note that the AIE of Cr complex correspond to the removal of an electron from the 3d orbitals, while those of the Sc, Ti, V, Mn, Fe, Co and Ni ones correspond to removal from

metal-ligand orbitals. For the neutral Mn complex with 18-MVE closed shell configuration, the ionization energy is large than that obtained for Cr with open shell of 17-MVE structure as discussed previously.⁴⁹ Interestingly to note that the computed AIE for the iron complex is comparable to that obtained in previous work¹⁷ and to that of the isoelectronic Mn(Bz)₂ complex.⁴³ The AEA values oscillate across the 3d series for the studied complexes (Fig. 8), i.e., they enhance from Sc (0.47 eV) to V (0.82 eV), afterwards they decrease from V to Cr (0.57 eV) and so on. The positive AEA values of M(Bz)Cp suggest that the anions are more stable than the corresponding neutrals and are found in the range 0.31-1.27 eV (BP86) or 0.10- (B3LYP) comparable to previous work.⁵⁰ For the vanadium and chromium complexes, the anionic species are obtained by adding an electron into the singly 33a' orbital, which is purely metallic, where the electron attachment is more sensitive to the electron density around the metal atom as discussed in previous work.⁴⁹ The largest value of 1.27 eV (BP86) obtained for the nickel complex is in accordance with the LUMO's (-1.34 eV) shift towards high levels, while the smallest AEA corresponds to the iron (0.31 eV) complex which matches very well with its lowest LUMO (-2.33 eV) energy. In light of these results, one can conclude that the iron complex is most easy to oxidize and to reduce contrary to the nickel one which is the most difficult to oxidize and to reduce, which could be considered as the most stable complex, however, the Sc, Ti, V, Cr, Mn and Co complexes are with an intermediate behaviour whose values are roughly comparable to those of metal benzene sandwich complexes.⁴⁷

5. Conclusion

In this work, we have explored the electronic and the molecular structure as well as the ionization energy and electron affinity for the first row transition metals sandwiched between benzene and cyclopentadienyl ligands. The reported results point out the richness of the coordination of the benzene and the cyclopentadienyl ligands. Thus, depending on the electron count and the nature of the metal the η^6 - η^5 , η^4 - η^5 , η^6 - η^2 and η^2 - η^5 coordination modes can be adopted by the benzene and the cyclopentadienyl ligands. The coordination lower than η^6 for the benzene are associated to distorted structures showing slippage towards the external carbon atoms. Indeed, it should be possible to observe the existence of several isomers of similar energy of different hapticities and their interconversion in solution. The local structures of the transition metal mixed sandwich complexes, have been studied by density functional theory calculations which predicted detailed of molecular structures giving the M-

C(Bz) bond distance slightly longer than that of M-C(Cp) for all the derivatives except for the $[\text{Fe}(\text{Bz})\text{Cp}]^+$ and $[\text{Ni}(\text{Bz})\text{Cp}]^+$ singlet and triplet spin state complexes. The structures optimized in their singlet state fulfilling the 18-electrons rule exhibit large HOMO-LUMO gaps, while the deficient ones (14- and 16-metal valence electrons) are characterized by moderate or small ones, particularly that of Vanadium.

The ionization energy of M(Bz)Cp complex across the 3d series are qualitatively different. In particular, the ionization energy steadily rises from Sc to Mn, while it drops suddenly from Mn to Fe, afterward it increases from Fe to Ni *via* Co.

We also provide results on electron affinities on systems for which no experiment exists. We hope that our work will stimulate further experimental and theoretical studies. We note the good agreement between the theoretical results and the available experimental data on the studied systems and explain all the trends.

Acknowledgment

We gratefully acknowledge support from the Algerian MESRS “Ministère de l’Enseignement Supérieur et de la Recherche Scientifique”.

Supplementary information.

Bond distances, energetic parameters and total bonding energies for the optimized geometries of the computed compounds (Tables S1-S4) BP86 and (Tables S5-S8) B3LYP.

References

- (1) T. J. Kealy and P. L. Paulson, *Nature*, 1951, **168**, 1039.
- (2) S. A. Miller, J. A. Tebboth and J. F. Tremaine, *J. Chem. Soc.*, 1952, **632**.
- (3) (a) J. E. Ellis, D. W. Blackburn, P. Yuen and M. Jang, *J. Am. Chem. Soc.*, 1993, **115**, 11616. (b) E. P. Kündig, C. Perret, S. Spichiger and G. J. Bernardinelli, *Organomet. Chem.*, 1985, **286**, 183. (c) E. O. Fischer, C. Elschenbroich and C. G. Kreiter, *J. Organomet. Chem.*, 1967, **7**, 481. (d) E. D. Brady, J. S. Overby, M. B. Meredith, A. B. Mussman, M. A. Cohn, T. P. Hanusa, G. T. Yee and M. Pink, *J. Am. Chem. Soc.*, 2002, **124**, 9556. (e) M. B. Meredith, J. Crisp, E. D. Brady, T. P. Hanusa, G. T. Yee, N. R. Brook, B. E. Kucera and V. G. A. Young Jr, *Organometallics*, 2006, **25**, 4945. (f) M. B. Meredith, J. A. Crisp, E. D. Brady, T. P. Hanusa, G. T. Yee, M. Pink, W. W. Brennessel and V. G. Young Jr, *Organometallics*. 2008,

- 27, 5464. (g) J. A. Crisp, R. M. Meier, J. S. Overby, T. P. Hanusa, A. L. Rheingold and W. W. Brennessel, *Organometallics*, 2010, **29**, 2322. (h) J. A. Crisp, M. B. Meredith, T. P. Hanusa, G. Wang, W. W. Brennessel and G. T. Yee, *Inorg. Chem*, 2005, **44**, 172. (i) S. Guo, B. I. alog, R. Hauptmann, M. Nowotny, J. J. Schneider, *J. Organomet. Chem*, 2009, **694**, 1027. (j) F. Chekkal, S.M.Zendaoui, B. Zouchoune, J-Y. Saillard, *New J. Chem*, 2013, **37**, 2293. (k) K. Jonas, B. Gabor, R. Mynott, A. K. ngermund, O. Heinemann and C.Krüger, *Angew. Chem*, 1997, **36**, 1712, (l) K. Jonas, P. Kolb, G. Kollbach, B. Gabor, R. Mynott, K. Angermund, O. Heinemann and C.Kruger, *Angew. Chem. Int. Ed. Engl*, 1997, **36**, 1714. (m) R. Gleiter, S. Bethke, J.Okubo, K.Jonas, *Organometallics*, 2001, **20**, 4274. (n) M. R. Churchill and K.K.G.Lin, *Inorg. Chem*, 1973, **12**, 2274. (o) S. Bendjaballah, S Kahlal, K. Costuas, E. Bevillon and J.-Y.Saillard, *Chem.-Eur. J*, 2006, **12**, 2048. (p) H. Korichi, F. Zouchoune, S.-M Zendaoui, B. Zouchoune and J.-Y. Saillard, *Organometallics*, 2010, **29**, 1693. (q) S. Farah, N. Bouchakri, S.M. Zendaoui, J.Y. Saillard and B. Zouchoune, *J. Mol. Struct*, 2010, **953**, 143. (r) A. Saiad and B. Zouchoune, *Can. J. Chem*, 2015, **93**: dx.doi.org/10.1139/cjc-2015-0104.
- (4) E. O. Fischer and W. Z. Hafner, *Naturforsch, Teil B*. 1955, **10**, 665.
- (5) M. T. Anthony, M. L. H. Green and D. Young, *J. Chem. Soc; Dalton Trans*. 1975, **1419**.
- (6) O. N. Krasochka, A. E. Shestakov, G. G. Tairova, Yu. A. Shvetsov, E. F. Kvashina, V. I. Onomarev, L. O. Atovmyan and Yu. G. Borod'ko, *Khim, Fiz*, 1983, **2**, 1459.
- (7) E. O. Fischer and W. Z. Hafner, *Naturforsch*, 1953, **8**, 444.
- (8) K. R. Flower and P. B. Hitchcock, *J. Organomet. Chem*, 1996, **507**, 275.
- (9) W. Goll, J. Miiller, *J. Organomer. Chem*, 1974, **71**, 257.
- (10) J. Ruiz, M. Lacoste and D. Astruc, *J. Am. Chem. Soc*, 1990, **112**, 5471.
- (11) D. Astruc, J. R. Hamon, G. Althoff, E. Román, P. Batail, P. Michaud, J. P. Mariot, F. Varre and D.Cozaq, *J. Am. Chem. Soc*, 1979, **101**, 5545.
- (12) W. Finckh, B. Z. Tang, A. Lough and I. Manners, *Organometallics*, 1992, **11**, 2904.
- (13) T. P. Gill and K. R. Mann, *Organometallics*. 1982, **1**, 485.
- (14) M. Shotaro and T. Mochida, *Organometallics*, 2013, **32**, 283.
- (15) J. L. Xia, W. C. Xiong, G. Chen, G. A. Yu, S. Jin and S. H. Liu, *Transition Met Chem*, 2009, **34**, 389.
- (16) K. Jonas, W. Russeler, K. Angermund and C. Kruger, *Angew. Chem. Int. Ed. Eng*, 1986, **25**, 927.
- (17) F. Ogliaro, J. F. Halet, D. Astruc and J. Y. Saillard, *New. J. Chem*, 2000, **24**, 257.

- (18) S. Farah, S. Ababsa, N. Benhamada and B. Zouchoune, *Polyhedron*, 2010, **29**, 2722.
- (19) N. Bouchakri, A. Benmachiche and B. Zouchoune, *Polyhedron*, 2011, **30**, 2644.
- (20) A. Benmachiche, S.M. Zendaoui, S.E. Bouaoud and B. Zouchoune, *Int. J. Quant. Chem*, 2012, **11**, 985.
- (21) S. Farah, H. Korichi, S.M. Zendaoui, J.Y. Saillard and B. Zouchoune, *Inorg. Chim. Acta*, 2009, **362**, 3541.
- (22) M. Merzoug and B. Zouchoune, *J. Organomet. Chem*, 2014, **770**, 69.
- (23) S.M. Zendaoui and B. Zouchoune, *Polyhedron*, 2013, **51**, 123.
- (24) A. Peng, X. Zhang, Q. S. Li, R. B. King and H. F. Scharfer III, *New. J. Chem*, 2013, **37**, 775.
- (25) H. Wang, R. B. King, H. F. Schaefer III, *Eur. J. Inorg*, 2008, 3698.
- (26) Q. Fan, H. Feng, W. Sun, H. Li, Y. Xie, R. B. King, H. F. Scharfer III, *New. J. Chem*, 2013, **37**, 1545.
- (27) *ADF2013.01*, Theoretical Chemistry, Vrije Universiteit: Amsterdam, The Netherlands, SCM.
- (28) E. J. Baerends, D. E. Ellis and P. Ros, *Chem. Phys*, 1973, **2**, 41.
- (29) G. te Velde and E. J. Baerends, *J. Comput. Phys*, 1992, **99**, 84.
- (30) C. Fonseca Guerra, J. G. Snijders, G. te Velde and E. Baerends, *J. Theo. Chim. Acc*, 1998, **99**, 391.
- (31) F. M. Bickelhaupt and E. J. Baerends, *Rev. Comput. Chem*, 2000, **15**, 1.
- (32) G. te Velde, F. M. Bickelhaupt, C. Fonseca Guerra, S. J. A. van Gisbergen, E. J. Baerends, J. G. Snijders and T. Ziegler, *J. Comput. Chem*, 2001, **22**, 931.
- (33) S. D. Vosko, L. Wilk and M. Nusair, *Can. J. Chem*, 1990, **58**, 1200.
- (34) A. D. Becke, *J. Chem. Phys*, 1986, **84**, 4524.
- (35) A. D. Becke, *Phys. Rev. A*, 1988, **38**, 3098.
- (36) J. P. Perdew, *Phys. Rev. B*, 1986, **33**, 8822-8824.
- (37) J. P. Perdew, *Phys. Rev. B*, 1986, **34**, 7406-7406.
- (38) Becke, A. D. *J. Chem. Phys.* **1993**, **98**, 5648.
- (39) Lee, C.; Yang, W.; Parr, R. G. *Phys. Rev. B: Condens. Matter Mater. Phys.* **1988**, **37**, 785.
- (40) L. Versluis and T. Ziegler, *J. Chem. Phys*, 1988, **88**, 322.
- (41) L. Fan and T. Ziegler, *J. Chem. Phys*, 1992, **96**, 9005.
- (42) L. Fan and T. Ziegler, *J. Chem. Phys*, 1992, **96**, 6937.

- (43) P. Flükiger, H. P. Lüthi, S. Portmann and J. Weber, *MOLEKEL, Version 4.3.win32 Swiss Center for Scientific Computing (CSCS)*, Switzerland, 2000-2001.
<http://www.cscs.ch/molekel/>.
- (44) A. Haaland, *Acta Chem. Scand*, 1965, **19**, 41.
- (45) E. Keulen and F. Jellinek, *J. Organomet. Chem*, 1996, **5**, 490.
- (46) S. Yu. Ketkov, G. K. Fukin and L. N. Zakharov, *J. Organomet. Chem*, 2002, **649**, 100.
- (47) D. A. Braden and D. R. Tyler, *Organometallics*, 2000, **19**, 1175.
- (48) T. D. Jaeger, D. van Heijnsbergen, S. J. Klippenstein, G. von Helden, G. Meijer and M. A. Duncan, *J. Am. Chem. Soc*, 2004, **126**, 10981.
- (49) K. Judai, M. Hirano, H. Kawamata, S. Yabushita, A. Nakajima and K. Kaya, *Chem. Phys. Lett*, 1997, **270**, 23.
- (50) T. Masubuchi, K. Ohi, T. Iwasa, A. Nakajima, *J. Chem. Phys*, 2012, **137**, 224305.

Table of contents

Fig. 1 Optimized geometries for Sc(Bz)Cp, [Ti(Bz)Cp]⁺, Ti(Bz)Cp and [Ti (Bz)Cp]⁻ complexes. The relative energies between isomers are given in (kcal/mol).

Fig. 2 MO diagrams of M(η^6 -Bz)Cp) (M = Sc, V) and [M(η^6 -Bz)Cp)]⁺ (M = Ti, Cr) complexes.

Fig. 3 Optimized geometries for V(Bz)Cp, [Cr(Bz)Cp]⁺, Cr(Bz)Cp and [Cr(Bz)Cp]⁻ complexes. The relative energies between isomers are given in kcal/mol.

Fig. 6 Optimized geometries for [M(Bz)Cp]^{+1/0/-1} (M = Mn, Fe) complexes. The relative energies between isomers are given in (kcal/mol).

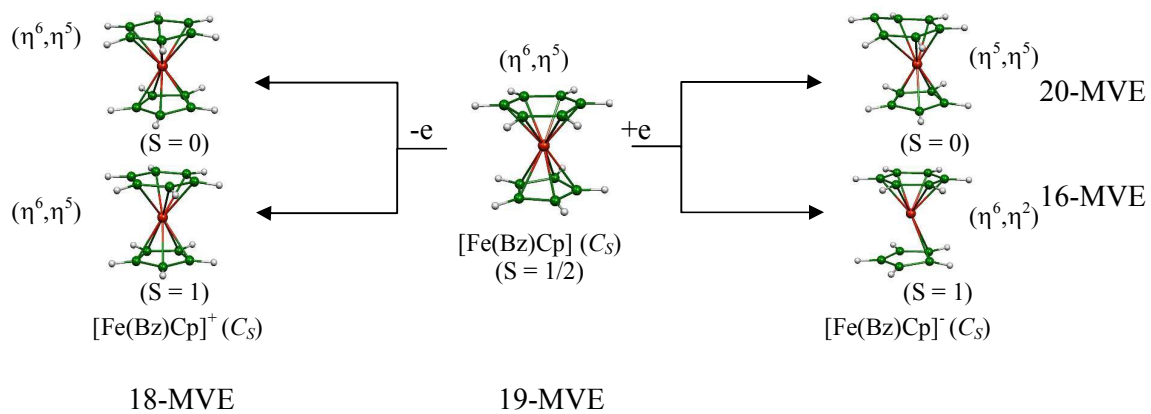
Fig. 5 MO diagrams of M(Bz)Cp (M = Mn, Co) and, [M(Bz)Cp]⁺ (M = Fe, Ni) complexes.

Scheme 1. Oxidation and reduction mechanisms for neutral iron (a), cobalt (b) and nickel (c) complexes.

Fig. 6 Optimized geometries for [M(Bz)Cp]^{+1/0/-1} (M = Co, Ni) complexes. The relative energies between isomers are given in (kcal/mol).

Fig. 7 Ionization energy variation as function of metal valence electrons.

Fig. 8 Electron affinity variation as function of metal valence electrons.



Depending on the electron count of the iron metal and the spin state of the complex, various coordination modes are adopted by the benzene and the cyclopentadienyl rings.

(c)